ISSN 1063-7729, Astronomy Reports, 2011, Vol. 55, No. 3, pp. 284–291. © Pleiades Publishing, Ltd., 2011.
Original Russian Text © V.N. Obridko, B.D. Shelting, I.M. Livshits, 2011, published in Astronomicheskii Zhurnal, 2011, Vol. 88, No. 3, pp. 313–320.

Open Magnetic Fields on the Sun and Solar Wind Parameters at the Earth's Orbit

V. N. Obridko*, B. D. Shelting, and I. M. Livshits

Pushkov Institute of Terrestrial Magnetism, the Ionosphere, and Radio Wave Propagation, Russian Academy of Sciences, Troitsk, Moscow Region, 142190 Russia

Received August 19, 2010; in final form, September 20, 2010

Abstract—It is shown that the parameters of the solar-wind magnetic field are determined by regions in coronal holes at distances of 1.1–1.4 solar radii, where the field lines are radial at low heights. Expanding further in a narrow nozzle or funnel, the field lines become radial throughout the unipolar region at 2.5 solar radii. Hence, the traditional approach of comparing the characteristics of the interplanetary field at the Earth's orbit and at the corresponding helio-projection point on the Sun is not quite correct. It gives good results for the signs and sector structure of the field; however, the magnitude of the field is formed in a more extensive area. Taking this into account, we can correlate the field values on the Sun with the interplanetary magnetic field (IMF), and thus explain the absence of weak fields in the vicinity of the IMF neutral line (the two-peaked nature of the distribution).

DOI: 10.1134/S1063772911030048

1. INTRODUCTION

In this study, we have compared data on the interplanetary magnetic field (IMF) with calculations based on observations of the Sun. The OMNI data for the IMF components downloaded from the NSSDC server (http://nssdc.gsfc.nasa.gov/omniweb) have been used.

There are currently three unsolved problems associated with comparisons of the solar and near-Earth fields [1, 2]:

(1) The low correlation of the absolute values and high correlation of the signs. The correlation between the field's radial components at the Earth's helio-projection point (HPP) on the Sun and on the corresponding field line near the Earth is usually very high. Under a closer examination, however, it becomes clear that this is due to the correlation of the field signs and not the field values (Fig. 1; note that the field signs on the Sun and in near-Earth space are defined in opposite ways). Essentially, we see two clouds of points in two anti–symmetric quadrants. When we compare the field absolute values, both clouds move to the first quadrant, and the correlation disappears. With the sign taken into account, the correlation coefficient is 0.93, while it is only 0.65 for the field absolute values.

(2) The second problem can be called the "puzzle of the two peaks." If we plot the field distribution at the Earth's HPP on the solar source surface and in the solar wind at the Earth's orbit, we obtain two completely different distributions (Fig. 2). Unlike the field distribution at the source surface, the histogram for the IMF has a well defined two-peaked shape. This difference holds for all components, even if we consider higher resolution data (up to hourly mean values), and its nature is quite unclear, since our basic picture of the solar wind suggests that the quiet solar wind should reproduce the source-surface field at the Earth's HPP to within a scale factor.

(3) According to basic concepts about the Sun, the magnetic field in the quiet solar wind originates from the source-surface field as a result of its radial expansion. In this case, the field in the solar wind at the Earth's orbit can readily be calculated by multiplying by the factor $(R_{SS}/R_E)^2$ (where R_{SS} and R_E are the heliocentric distances to the solar source surface and to the Earth). Including the recalculation from microTesla to nanoTesla, this factor is 0.142. According to this basic concept, multiplying the source-surface field B_{SS} by this factor should yield values close to the measured ones, and we should obtain a regression equation with a scale factor equal to unity. In reality, the calculated field values are very small (Figs. 1 and 2), and must be multiplied by an additional scale factor exceeding unity in order for them to be comparable to the measured field.

Note that all three problems are present in the standard calculation method, which assumes that the magnetic fields are potential and current-free up

*E-mail: obridko@izmiran.ru

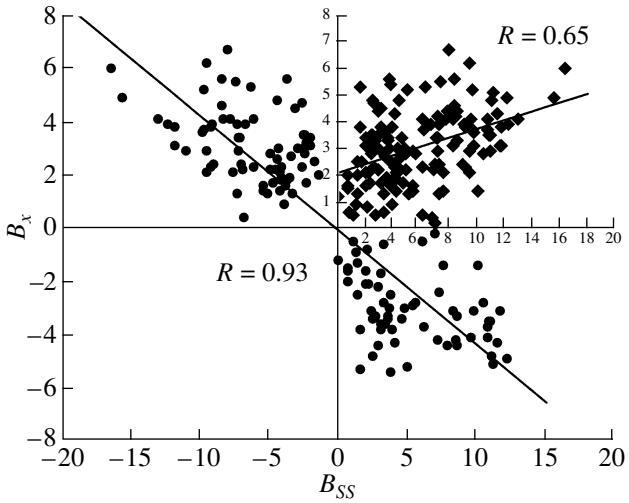

Fig. 1. Correlation between B_X and the source-surface field B_{SS}, taking into account the signs of both values (second and fourth quadrants), and the correlation between their absolute values (first quadrant, upper right panel). The time shift is four days.

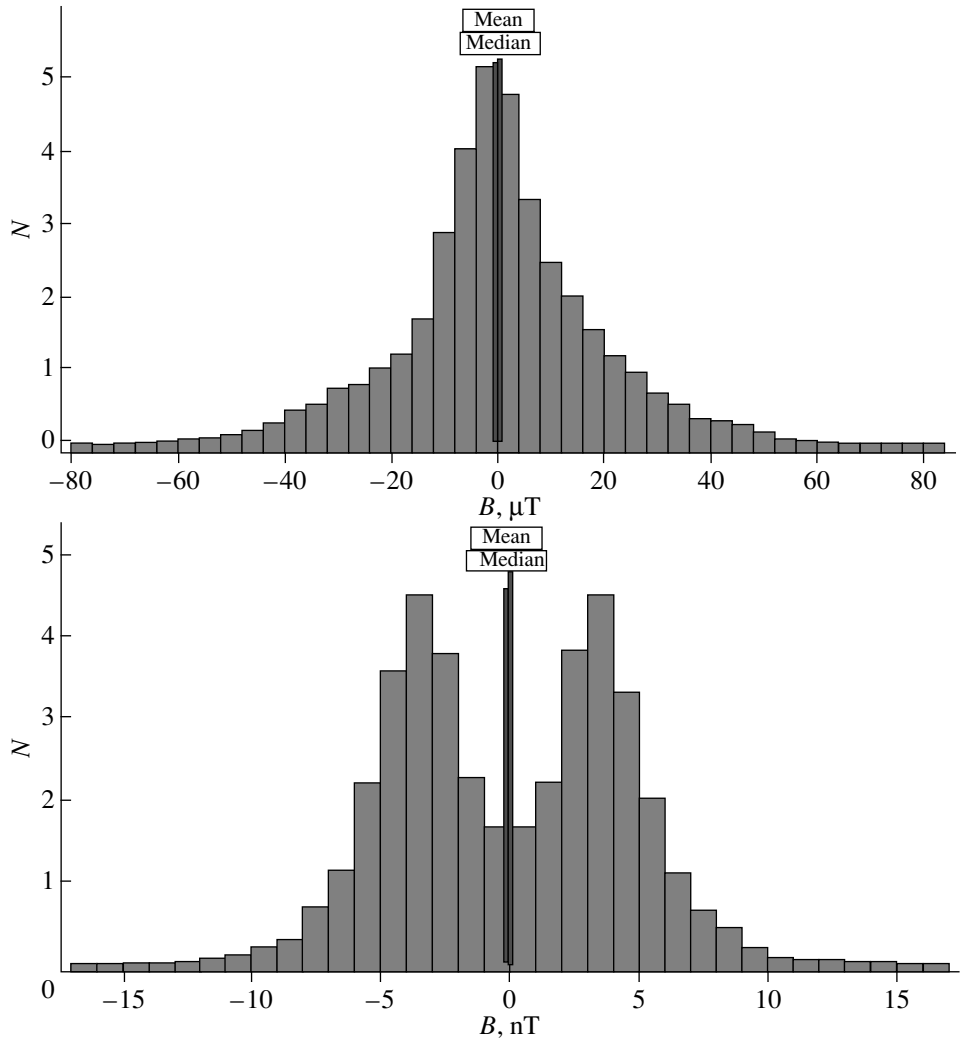

Fig. 2. Histograms of distribution of the source-surface field B_{SS} (top) and the IMF at the Earth's orbit (bottom).

Number of CHs for each year

Year	Number of CHs
1998	14
1999	28
2000	23
2001	28
2002	37
2003	46
2004	39
2005	25
2006	27
2007	31
2008	22
2009	18

to the source surface. Therefore, only the first few harmonics remain at large heights, the main of these being the dipolar field. Beginning from a certain height, the field then decays as R^{-3}, similar to a dipolar field. The regime then changes abruptly: the structure is completely controlled by the solar outflow, the field lines become fully open, and the field depends on the distance as R^{-2}. We traditionally associate the field in the heliosphere and at the Earth's orbit with the field at the Earth's HPP. In doing so, we ignore the fact that, though the source-surface field is fully open, the fields at lower heights are rooted in coronal holes (CHs).

Wang et al. [3] identify CHs with regions of open field lines, and use both terms equally. However, the situation is not so simple. Even the most recent calculations do not confirm that these two phenomena are identical [2, 4, 5]. Although the inter-relation between CHs and regions of open field seems logical in principle, there remain some unclear areas. In particular, Stepanyan [4] noted a difference in the spatial distribution of CHs and large-scale (background) magnetic fields over a solar cycle.

There is no doubt that high-speed streams are associated with CHs and IMF sector boundaries [6–10]. However, they cover much larger areas than CHs. The eastern boundary of the solar-wind high-speed streams lies in the transition zone with a width of 40°–50° between the CHs and the boundary of the IMF sector structure. From 75% to 90% of the eastern boundaries of the high-speed streams are 25°–30° westward of the IMF sector structure.

It is usually believed that CHs expand "super-radially" [11–13]; i.e., the field lines in this region depart significantly from the radial direction characteristic of a magnetic monopole. This is because the field lines all over the source surface originate from open fields associated with CHs, which occupy only a small area in the lower corona and chromosphere. However, here again, the situation is not so simple. In fact, the super-radial expansion in the central part of a large CH begins at a height of 1.4 solar radii from the center of the Sun. The CH field below this level is strictly radial, unlike the ambient closed field [2, 5, 14].

Thus, we have adopted a scheme similar to that proposed by Wang et al. [15] to explain radio observations of CHs, represented in their Fig. 2.

The space between the closed fields is occupied by open magnetic field (OMF). At the center of the OMF up to the height of 0.4–0.6 solar radii is a zone of radial magnetic field (RMF), observed as a CH in X-rays, the extreme ultraviolet, and the He I 10 830 Å line [2, 5]. Thee is an enhancement of the radio emission at meter and decameter wavelengths in this zone [15]. At the periphery of the OMF zone, in the vicinity of the closed field, we can see the super-radial expansion. Thus, we have two OMF zones out to 0.4 solar radii—a zone of radial field at the center and a transition zone at the periphery.

2. DATA AND CALCULATION METHODS

We used the 1024 × 1024 SOHO data in FITS format downloaded from the Internet (http://sohowww.nascom.nasa.gov/cgi-bin/summary_query_form). For our detailed analysis, we used the data from the site http://umbra.nascom.nasa.gov/eit/eit-catalog.html with the Solarsoft program eit_prep downloaded from the site fttp://sohowww.nascom.nasa.gov/solarsoft/soho/eit/idl/anal/eit_prep.pro. A catalog of CHs for 1998–2009 was compiled. From the beginning of 1998 to the end of 2002, the CHs were selected based on their configurations (a simple oval shape far from other CHs) and positions (near the center of the disk). The data were taken from the Solar Geophysical Data "Coronal Hole Daily Maps (NSO/RP)," which represent daily data, naturally, subject to the weather conditions. The list of coronal holes from 2003 to October 2009 was taken from the site http://www.dxlc.com/solar/coronal_holes.html, "Coronal hole history (since late October 2002)." Calculations were made for all CHs whose passage across the disk was not accompanied by halo coronal mass ejections (CMEs). The data on full-halo CMEs were taken from the catalogs of Gopalswami

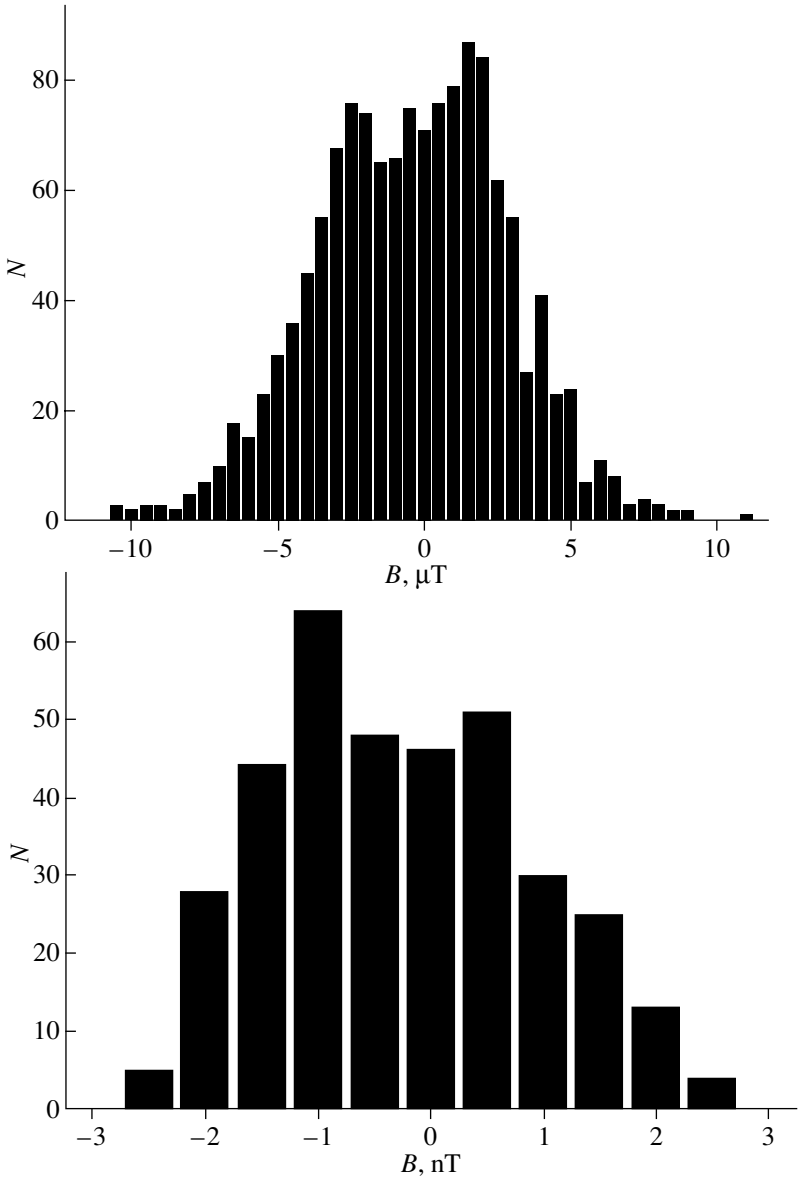

Fig. 3. Histograms of the sector mean field at the source surface (top) and the IMF at the Earth's orbit (bottom).

(http://cdaw.gsfc.nasa.gov/CME_list/HALO/halo.html).

After the above comparison, we selected 338 CHs. The table presents the number of CHs for each year in our catalog.

We analyzed 284 Å SOHO images of the Sun. A brightness equal to 0.25 of the annual mean total solar brightness at this wavelength was adopted for the photometric boundaries of CHs. The procedure used to acquire the data is described in more detail in [14]. Comparison with the magnetic-field structure was done using data from the John Wilcox Solar Observatory (WSO). The calculation method used has been described in literature many times (e.g., see [16, 17]). We used classical harmonic coefficients; i.e., the field in the photosphere was not assumed to be radial. All calculations included ten harmonics in the expansion.

3. COMPARISON WITH THE FIELD AVERAGED OVER EXTENSIVE AREAS

We have suggested that the observed two-peaked distribution is due to the fact that the IMF sign and magnitude are associated with different regions on the solar surface. The sign is controlled by the IMF sector structure, which, in turn, reflects the B_{SS} sign reversal at the Earth's HPP, while the field amplitude is integrated over an entire sector of one sign.

To verify this suggestion, we averaged the B_{SS} daily values calculated within a circle of radius R_0

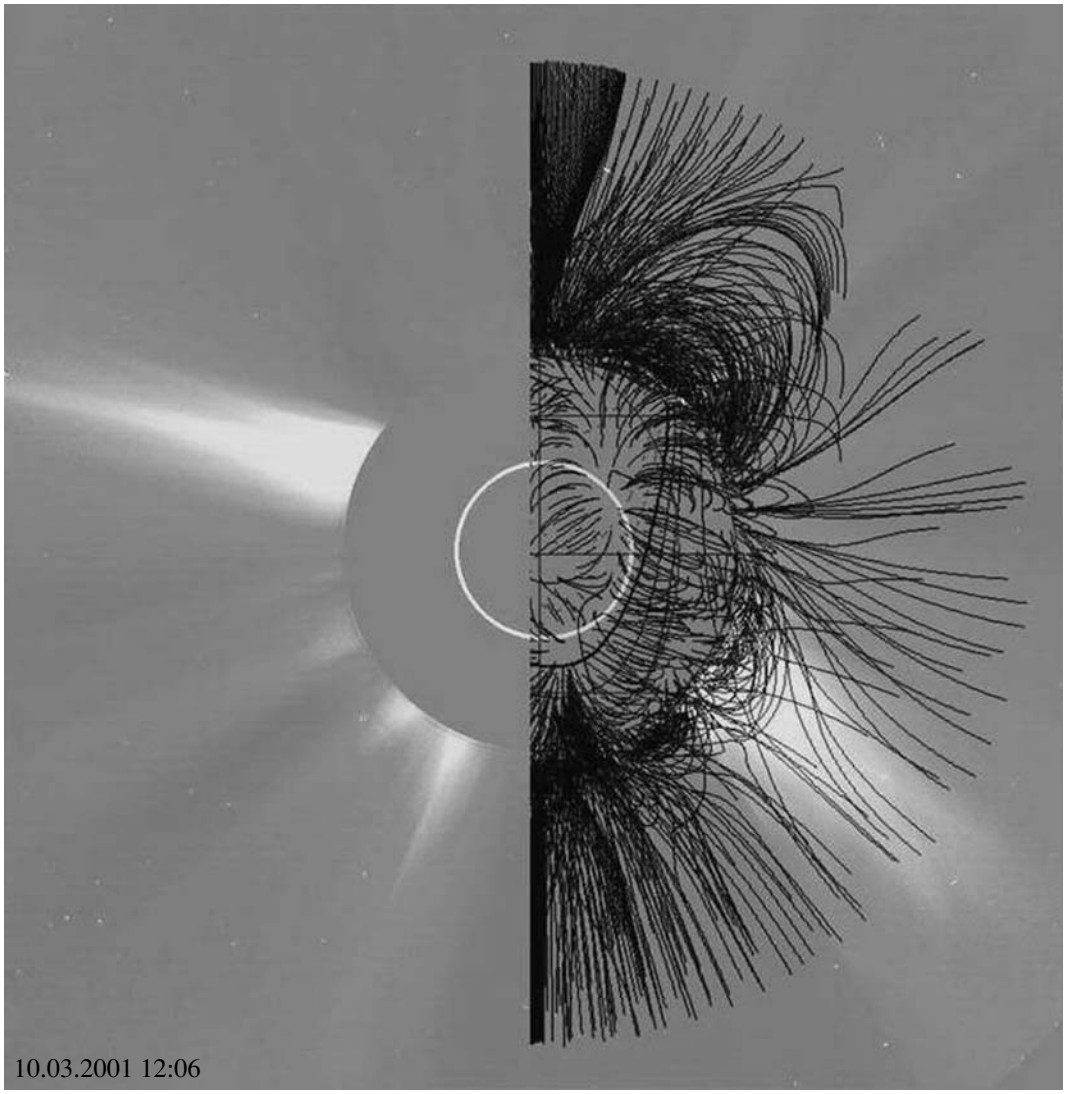

Fig. 4. Coronal hole at the eastern limb and magnetic-field lines.

around the Earth's HPP for 2005. The calculations were performed for $R_0 = 0°$, 15°, 25°, 40°, and 70°. The values obtained were then compared with the daily values of B_L, with a shift of four days. The resulting correlation is fairly high ($\sim$0.70) out to $R_0 = 40$. With further increase in R_0, the correlation decreases abruptly. This is easy to understand, since the upper boundary of the heliospheric current sheet did not extend above 40° in 2005, so that we pass beyond the unipolar sector at $R_0 > 40°$. The main thing this procedure has shown is that the two-peaked distribution forms right on the Sun, with the asymmetry coinciding with that observed at the Earth's orbit, bearing in mind that the X axis has opposite directions on the Sun and in the IMF (see Fig. 3). At the same time, the histogram of the source-surface field at the Earth's HPP ($R_0 = 0$) has a single peak, as in Fig. 2, and corresponds to a simple Gaussian distribution. Of course, this is not the only possible explanation. Such a disappearance of the fields near the zero point could be due to various non-stationary effects and discontinuities in the solar wind in the vicinity of the neutral line. Note that the horizontal axes in Figs. 2 and 3 are in μT for the source surface and in nT for the IMF. To bring these data to a single system, we had to multiply the field values on the Sun by 0.142. The the calculated field then remains underestimated, and averaging over an extensive area does not improve the situation.

4. COMPARISON WITH THE FIELD AVERAGED OVER A CORONAL HOLE

In order to avoid the inconsistency indicated above, we compared the IMF with the mean magnetic-field values obtained under different averaging conditions. The calculations were based on the idea

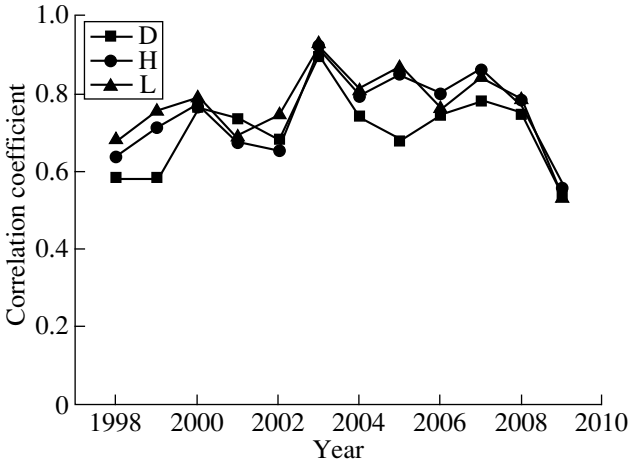

Fig. 5. Correlation between three different calculations of the near-Earth field and the measured field. The calculations shown are versions 1 (squares, D), 2 (circles, H), and 3 (triangles, L).

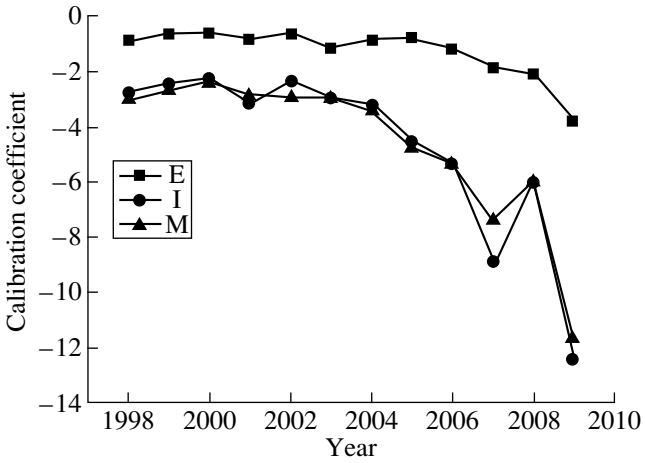

Fig. 6. Calibration coefficient used to compare three versions of the calculated near-Earth field with the measured field. The calculations shown are versions 1 (squares, E), 2 (circles, I), and 3 (triangles, M).

that the darkest part of a CH corresponds to the region where the field becomes radial at 1.1–1.4 solar radii. The result is illustrated in Fig. 4, using the SOHO/LASCO–C2 image of March 10, 2001 as an example. This figure displays a CH in the equatorial region at the western limb. The magnetic-field lines calculated applying a potential approximation are superimposed on the solar image. The field lines in the central, darkest part of the CH become radial very low in the corona.

Four different values were calculated.

1. The mean field at 1.1 solar radii in the dark part of the hole. This and the following two procedures were performed for all 338 CHs in the catalog. The values obtained were compared with the IMF and density, taking into account the transport time of three to four days.

2. The field at 2.5 solar radii (i.e., at the source surface) in the darkest part of the CH.

3. The field at the disk center. Here, the source-surface magnetic field at the Earth's HPP was calculated for each day of observation of the CH.

4. The mean field at various heights (from 1 to 2.2 solar radii) for all CHs observed in 2005.

To compare numerically the solar and near-Earth interplanetary magnetic fields (the OMNI data), we recalculated the mean fields obtained for a distance of 1 AU using a radial propagation model. The mean field B_r was multiplied by 0.0274 if initially calculated at 1.1 solar radii and by 0.142 if initially calculated at the source surface (2.5 solar radii) (see Fig. 5).

In the first three cases, the correlation between the measured and calculated values is fairly high: of order 0.8, on average, or even higher in some years.

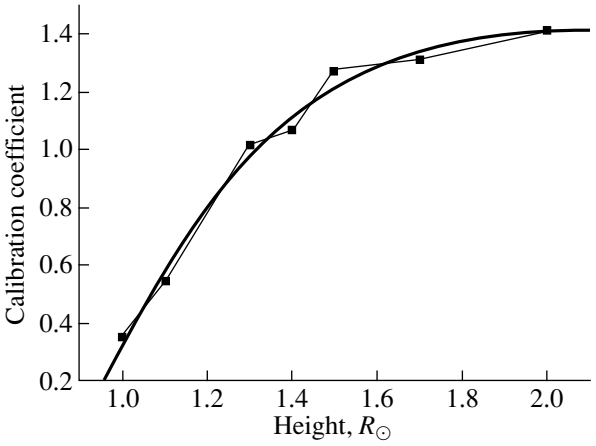

Fig. 7. Calibration coefficient as a function of height in the CHs. The approximating curve is also plotted.

However, we must not assign this too much importance, because this again represents a correlation of the field signs, which essentially reflects a correlation between the sector structures in the Sun and the IMF. This is why the correlation decreases at the end of the period under consideration: at the cycle minimum, the heliospheric current sheet flattens and the sectors disappear. We performed our calculations for a transport time of four days, since a shift of three days gives a lower correlation.

The difference between the first three values becomes much larger when the calibration coefficient is calculated. The coefficient required to bring the measured and calculated values to a single scale should be close to unity. However, in all cases when the initial magnetic field was taken at 2.5 solar radii (cases 2 and 3), the coefficient required to match the field recalculated to 1 AU with the measured IMF was much higher than unity. On the other hand, the calculations for an initial height of 1.1 solar radii (case 1) yield an average coefficient of 0.93 (see Fig. 6; the calibration coefficients are negative due to the difference in the positive directions for the field on the Sun and in the IMF).

The aim of the fourth calculation was to ascertain the height where the field lines in a CH became completely open. While the other calculations were made for 1.1 solar radii (the height at which the 284 Å line is presumably emitted), here, we calculated the calibration coefficient for a variable "source-surface" height. We found that the angular coefficient in the regression equation is close to unity at 1.2–1.4 solar radii (Fig. 7).

5. CONCLUSIONS

The magnetic field carried to the Earth by the solar wind does not form at the Earth's helio-projection point, but instead in a more extensive area from −40° to +40°. Its generation is controlled mainly by CHs located at the centers of "bays" of the neutral line of a definite sign.

As a result, the solar-wind field at the Earth's orbit is determined by streams coming from an extensive area on the Sun. Accordingly, the spread of the field magnitudes is very large, and the correlation between the calculated and measured values is low (see Section 1, Fig. 1).

Since the field is formed in a broad region, there is a natural drop in the field values in the vicinity of the neutral line (forming a two-peaked distribution). This is contrary to what we see if the field at the HPP is considered.

The asymmetry of the distribution of the IMF has a solar origin, and its sign agrees with the sign of the distribution of the solar field averaged over an extensive area.

The high-speed stream is formed entirely at the base of its CH. The solar-wind parameters are determined at the height where the field lines in the CH are radial. The CH acts as a nozzle ejecting the stream. Similar conclusions were drawn in [18–21], which compared SOHO/SUMER Doppler velocities measured in the SiII (153.3 nm), CIV (154.8 nm), and NeVIII (77.0 nm) emission lines with the extrapolated magnetic field. These studies showed that the solar-wind streams escape from narrow "funnels" from a height of about 20 Mm.

ACKNOWLEDGMENTS

The work was supported by the Russian Foundation for Basic Research (project code 08-02-00070).

REFERENCES

1. O. I. Bugaenko, I. A. Zhitnik, A. P. Ignat'ev, et al., Izv. Krymsk. Astrofiz. Observ. **100**, 136 (2004).
2. E. I. Mogilevsky, V. N. Obridko, and N. S. Shilova, Solar Phys. **176**, 107 (1997).
3. Y.-M. Wang, S. H. Hawley, and N. R. Sheeley, Science **271**, 464 (1996).
4. N. N. Stepanyan, Izv. RAN, Ser. Fiz. **59**, 63 (1995).
5. V. N. Obridko, in *Advances in Solar Connection with Interplanetary Phenomena,* Ed. by X. Feng, F. Wei, and M. Dryer (Intern. Acad. Publ., Beijing, 1998), p. 41.
6. V. N. Obridko and B. D. Shelting, Geomagn. Aeron. **27**, 197 (1987).
7. V. N. Obridko and B. D. Shelting, Geomagn. Aeron. **27**, 660 (1987).
8. V. N. Obridko and B. D. Shelting, Kinem. Fiz. Nebesn. Tel **4**, 29 (1988).
9. V. N. Obridko and B. D. Shelting, Solar Phys. **124**, 73 (1989).

10. V. N. Obridko and B. D. Shelting, Astron. Zh. **67**, 890 (1990) [Sov. Astron. **34**, 449 (1990)].
11. V. A. Kovalenko, *Solar Wind* (Nauka, Moscow, 1983) [in Russian].
12. Y.-M. Wang and N. R. Sheeley, Jr., Astrophys. J. **355**, 726 (1990).
13. Y.-M. Wang, N. R. Sheeley, Jr., and A. G. Nash, Nature **347**, 439 (1990).
14. V. N. Obridko, B. D. Shelting, I. M. Livshits, and A. B. Asgarov, Solar Phys. **260**, 191 (2009).
15. Zh. Wang, M. R. Kundu, and H. Yoshimura, in *Solar and Stellar Coronal Structure and Dynamics,* A89–20526 06–92 (National Solar Observatory, Sunspot, NM, 1988), p. 458.
16. J. T. Hoeksema and P. H. Scherrer, *Solar Magnetic Fields—1976 through 1985*, UAG Report No. 94 (WDCA, Boulder, USA, 1986).
17. V. N. Obridko and B. D. Shelting, Solar Phys. **187**, 185 (1999).
18. C.-Y. Tu, C. Zhou, E. Marsch, et al., Science **308**, 519 (2005).
19. C.-Y. Tu, C. Zhou, E. Marsch, et al., in *Connecting Sun and Heliosphere Whistler,* ESA SP-592 (Eur. Space Agency, 2005), p. ??.
20. J.-S. He, C. -Y. Tu, and E. Marsh, Solar Phys. **250**, 147 (2008).
21. H. Tian, E. Marsch, W. Curdt, and J. He, archiv:0909.0739v1 [astro-ph.SR] (2009).

Translated by V. Obridko